

Mid-sagittal Plane and Mid-sagittal Surface Optimization in Brain MRI Using a Local Symmetry Measure

Mikkel B. Stegmann^{a,b}, Karl Skoglund^{a,b}, Charlotte Ryberg^b

^aInformatics and Mathematical Modelling, Technical University of Denmark,
Richard Petersens Plads, Building 321, DK-2800 Kgs. Lyngby, Denmark

^bDanish Research Centre for Magnetic Resonance,
Copenhagen University Hospital Hvidovre, Kettegård Allé 30, DK-2650 Hvidovre, Denmark

ABSTRACT

This paper describes methods for automatic localization of the mid-sagittal plane (MSP) and mid-sagittal surface (MSS). The data used is a subset of the Leukoaraiosis And DISability (LADIS) study consisting of three-dimensional magnetic resonance brain data from 62 elderly subjects (age 66 to 84 years). Traditionally, the mid-sagittal plane is localized by global measures. However, this approach fails when the partitioning plane between the brain hemispheres does not coincide with the symmetry plane of the head. We instead propose to use a sparse set of profiles in the plane normal direction and maximize the local symmetry around these using a general-purpose optimizer. The plane is parameterized by azimuth and elevation angles along with the distance to the origin in the normal direction. This approach leads to solutions confirmed as the optimal MSP in 98 percent of the subjects. Despite the name, the mid-sagittal plane is not always planar, but a curved surface resulting in poor partitioning of the brain hemispheres. To account for this, this paper also investigates an optimization strategy which fits a thin-plate spline surface to the brain data using a robust least median of squares estimator. Albeit computationally more expensive, mid-sagittal surface fitting demonstrated convincingly better partitioning of curved brains into cerebral hemispheres.

1. INTRODUCTION

The human brain consists on a coarse level of the cerebrum, the cerebellum and the brainstem. Most prominent is the cerebrum which is divided into hemispheres, connected by the nervous fiber bundle called the corpus callosum. The surface partitioning this approximate bilateral symmetry of the cerebrum is typically denoted *the mid-sagittal plane* (MSP) referring to its relative alignment with the sagittal plane of the human body.

Knowing the exact location of this surface has many applications. One is to provide the first step in spatial normalization or anatomical standardization of brain images.¹⁻³ Another is to provide means for estimating the departures from bilateral symmetry in the cerebrum^{1,4-6} often seen in pathological brains.⁵

Finally, determining the MSP is an invariable prerequisite for measurements on structures defined via this plane such as the MSP cross-section of the corpus callosum. A structure particularly interesting due to the many neurological studies indicating relationships between the size and shape of the corpus callosum, and gender, age, neurodegenerative diseases et cetera.⁷⁻⁹ MSP estimation can thus be viewed as a step prior to automated corpus callosum morphometry (cf.^{7,10-12}).

This paper presents two inherently three-dimensional methods for automatic localization of this partitioning surface using direct optimization of a local symmetry measure. Insisting on local symmetry contrary to global, which is the typical approach to MSP estimation, enables determination of brain symmetry that departs from head symmetry. The first method parameterizes a *mid-sagittal plane* and optimizes symmetry using the well-known Nelder-Mead simplex optimization scheme. The second utilizes results from robust statistics to fit a *mid-sagittal surface* (MSS) parameterized by thin-plate kernel functions. The efficacy of both methods is evaluated on magnetic resonance scans of a cohort of 62 elderly subjects, obtained from the pan-European LADIS study.¹³

Corresponding author is M. B. Stegmann, E-mail: mbs@imm.dtu.dk, Web: <http://www.imm.dtu.dk/~mbs/>.

2. RELATED WORK

Several papers have dealt with MSP estimation. The bulk part treats the problem as an optimization of global symmetry^{2,3,5,14-17} resulting in solutions dominated by the skull shape. However, Ardekani et al.¹ modified a global solution by introducing a thresholding approach aiming at excluding background and parts with non-overlapping skull.

Although being a truly three-dimensional problem, some choose to seek solutions in a two-dimensional fashion^{5,6} and later fusing these into a global solution, occasionally depending on various thresholds and other parameters that are hard to choose (see e.g. ref⁶). We note that two-dimensional approaches induce an implicit requirement of having 2D image slices with near-orthogonal orientation with respect to the MSP.

To the best of our knowledge, all previous approaches, but two, model the partitioning surface between the cerebral hemispheres as a plane. Christensen et al.¹⁸ and Darvann et al.¹⁹ assess dysmorphologies using the craniofacial MSP modeled as a thin-plate spline surface. Aiming at measuring craniofacial rather than brain asymmetry in infants with unilateral coronal craniosynostosis, this surface was fitted directly to landmark points placed manually on computed tomography scans of the skull.

3. DATA MATERIAL

The data material used in this study comprises 62 magnetic resonance images (MRI) of the human brain obtained from 62 elderly subjects (age 66 to 84 years) using a whole body MR scanner; Siemens Vision 1.5 Tesla. All subjects originated from a subset of the LADIS study¹³ (Leukoaraiosis and Disability in the Elderly). MR pulse sequence: MPRAGE; matrix size: 256×256 pixels; field of view: 250×250×150 mm (voxel size: 0.997×0.977×1.0 mm). A method for automatically locating the corpus callosum has previously been reported on a subset of the data set mentioned above.^{12,20}

4. METHODS

As not all literature is in consensus regarding the understanding of the mid-sagittal plane and surface, we will make these issues explicit by providing the following definitions:

DEFINITION 4.1. The mid-sagittal plane (MSP) is the planar surface which bisects the cerebrum into two cerebral hemispheres at their point of bilateral symmetry.

DEFINITION 4.2. The mid-sagittal surface (MSS) is the general surface which separates the cerebrum into two cerebral hemispheres at their point of bilateral symmetry.

It follows that the MSP and MSS must be placed exactly in the center of the inter-hemispheric fissure. This eliminates the extra degrees of freedom introduced in subjects with widened longitudinal fissures, and yields a unique MSP and MSS.

4.1. Mid-sagittal Plane Estimation

Due to the definition above, MSP estimation strategies based on global measures of symmetry must be rejected. This work is concerned about brain partitioning, rather than head symmetry. To avoid the complex, laborious and orientation-dependent methods induced by a slice-based approach to MSP estimation, the problem is cast into a standard optimization framework, requiring a suitable parameterization, a cost-function and an efficient optimizer. The parameterization should uniquely determine the orientation and position of the MSP, and the cost-function should estimate the local symmetry around the MSP.

This work employs a three-element parameterization of the MSP,

$$\mathbf{p} = [\theta \ \phi \ d]^\top, \quad (1)$$

where θ and ϕ are spherical coordinates (azimuth and elevation angles) determining the orientation of the plane and d is the perpendicular distance from the plane to the origin, determining the plane position.* Due to a cost-function consisting of local measurements, the initial MSP estimate, \mathbf{p}_0 , must be in the vicinity of the optimal MSP, \mathbf{p}_{opt} . This means that the origin of the spherical coordinates easily can be chosen so that no gimbal lock problems occurs.

The symmetry measure considered here resembles the cross-correlation, cc , between two discrete signals \mathbf{x} and \mathbf{y} of equal length

$$cc = \frac{(\mathbf{x} - \bar{\mathbf{x}})^\top (\mathbf{y} - \bar{\mathbf{y}})}{\sqrt{(\mathbf{x} - \bar{\mathbf{x}})^\top (\mathbf{x} - \bar{\mathbf{x}})} \sqrt{(\mathbf{y} - \bar{\mathbf{y}})^\top (\mathbf{y} - \bar{\mathbf{y}})}}. \quad (2)$$

Recalling that $cc \in [-1; 1]$, with $\mathbf{x} = L(-\mathbf{y})$ and $\mathbf{x} = L(\mathbf{y})$, [$L(\mathbf{y}) = \alpha \mathbf{y} + \beta$, $\alpha > 0$], at the limits respectively, cc can easily be modified to estimate the symmetry of a signal $\mathbf{z} = [\mathbf{x}^\top \ \tilde{\mathbf{y}}^\top]^\top$, where $\tilde{\mathbf{y}}$ is equal to \mathbf{y} with a reversed ordering of elements. Let $\mu = \bar{\mathbf{z}} = (\bar{\mathbf{x}} + \bar{\mathbf{y}})/2$, then a symmetry measure $s \in [0; 1]$ can be stated as

$$q(\mathbf{z}) = \frac{(\mathbf{x} - \mu)^\top (\mathbf{y} - \mu)}{\sqrt{(\mathbf{x} - \mu)^\top (\mathbf{x} - \mu)} \sqrt{(\mathbf{y} - \mu)^\top (\mathbf{y} - \mu)}}, \quad (3)$$

$$s(\mathbf{z}) = \max(0, q(\mathbf{z}))^2. \quad (4)$$

Notice that q is squared to emphasize strong symmetries. The symmetry at a given point of a plane is calculated from the set of image samples, \mathbf{z} taken from the line (incident with the plane normal) with end points having a distance of w on either side of the plane.

The joint symmetry for the entire plane, $S(\mathbf{p})$, is the sum of the symmetries for image samples obtained from a set of spatially equally distributed plane normals, $\{ \mathbf{z}_i \}_{i=1}^N$:

$$S(\mathbf{p}) = \sum_{i=1}^N s(\mathbf{z}_i). \quad (5)$$

The above cost-function is fed into a standard Nelder-Mead simplex optimizer (see e.g.²¹) to obtain the optimal MSP,

$$\mathbf{p}_{opt} = \arg \max_{\mathbf{p}} S(\mathbf{p}). \quad (6)$$

Although the simplex optimizer suits this low-dimensional problem well, other optimizers may also be considered. The signal intensities of \mathbf{z} is obtained using standard tri-linear interpolation of the voxel volume.

To gain larger convergence support and robustness towards local minima, a multi-scale formulation is applied where the normal width, w , is decreased with increasing iterations, while the simplex step-size is decreased as well.

This approach is thus inherently sensitive to a reasonable initialization. The rough in-scanner alignment should be sufficient, however if this is not the case, a straight forward initialization can be obtained from the principal axes of the voxel volume, e.g. as described in by Tuzikov et al.^{2,3}

*The origin is here chosen as the center of the voxel volume.

4.2. Mid-sagittal Surface Estimation

The mid-sagittal plane estimate is satisfyingly accurate for the great majority of subjects. Furthermore, in technical applications, it is reasonable to believe that planar cross-sections of the brain are favored. Nevertheless, a few of the patients in the present data set exhibit a slight but clearly visible bending along the entire mid-sagittal fissure, or, in some cases, a more prominent bending of the occipital lobe, proximal to the cerebellum (the so-called *torque effect*¹⁵). The optimal MSP cannot accurately represent the mid-sagittal surface (MSS, see Definition 4.2) in these cases. As shown by,¹⁸ a curved MSS may also be a result of craniofacial dysmorphologies. To account for these cases, we have investigated the possibility of fitting a surface instead of a plane using a similar symmetry measure as described above.

4.2.1. Surface Representation

Thin-plate splines are a natural choice of surface representation, since we are interested in capturing global curvature trends of the MSS. Thin-plate splines are able to contain such information using a low number of control points. The following basic description of thin-plate splines stems from.²²

A single thin-plate spline is the solution to the mechanical problem of finding the shape of an infinitely large and thin metal plate, minimizing its bending energy subject to interpolation of height values $y = f(x, z)$.

$$f(x, z) = a_1 + a_x x + a_z z + \sum_{i=1}^p w_i U(\|(x_i, z_i) - (x, z)\|) \quad (7)$$

Here, p is the number of *knots*, (x_i, z_i) on the two-dimensional manifold spanned by the imaginary steel plate. The corresponding values y_i can be interpreted as height values at the knots. $U(\|(x_i, z_i) - (x, z)\|)$ is the basis function $U(r) = r^2 \log r$, $U(0) = 0$. It can be shown that this choice leads to minimal plate bending energy.²⁴ The thin-plate spline consists of an affine part determined by the coefficients a_1 , a_x and a_z and a non-affine part where $\{w_i | i = 1 \dots p\}$ is a set of weights. We require that

$$\sum_{i=1}^p w_i = \sum_{i=1}^p w_i x_i = \sum_{i=1}^p w_i z_i = 0 \quad (8)$$

Since the thin-plate spline is an interpolant, we also have the p conditions $y_i = f(x_i, z_i)$. These conditions can be arranged in a linear system as

$$\begin{bmatrix} \mathbf{K} & \mathbf{P} \\ \mathbf{P}^\top & \mathbf{O} \end{bmatrix} \begin{bmatrix} \mathbf{w} \\ \mathbf{a} \end{bmatrix} = \begin{bmatrix} \mathbf{y} \\ \mathbf{o} \end{bmatrix} \quad (9)$$

where $K_{ij} = U(\|(x_i, z_i) - (x_j, z_j)\|)$, the i th row of \mathbf{P} is $(1, x_i, z_i)$, \mathbf{O} and \mathbf{o} are the 3×3 and 3×1 zero matrices respectively, and \mathbf{w} , \mathbf{y} and \mathbf{a} are column vectors formed from w_i , y_i and the affine coefficients. The design matrix in the linear system above is nonsingular provided that \mathbf{K} is invertible,²⁴ and the system can thus be solved by matrix inversion. A regularization term λ can be added so that the spline approximates the data points instead of interpolating them. This lowers the bending energy of the system. This is performed by changing \mathbf{K} into $\mathbf{K} + \lambda \mathbf{I}$, where \mathbf{I} is the $p \times p$ identity matrix.

The physical properties of the thin-plate spline suit our purposes fine. It will interpolate or approximate any points that have been found to lie on a potential MSS, without introducing excessive bending or sudden kinks in the surface.

The principal idea of the spline fitting algorithm is to first gather a set of data points in \mathbb{R}^3 which represents the mid-sagittal surface. Among these points, there will be many outliers. The spline is therefore fitted to data in a robust fashion.

4.2.2. Extraction of MSS Data Points

Assuming that the brain data is roughly aligned, it is possible to find reasonably accurate estimations of points on the MSS by finding the maximal local symmetry in a slice-by-slice, scanline fashion. Restricting the search to slices roughly containing the entire cerebrum, data points are found in the following way.

Algorithm 1 MSS Data Extraction

```
1: for each slice do
2:   for each scale do
3:     for each line do
4:       Slide a profile (of width  $k$ )  $s$  pixels across the midpoint:
5:       for each position do
6:         Compute the correlation coefficient between the first half of the profile
7:           and a mirrored version of the second half
8:         Measure the image intensity at the profile's center pixel
9:         Combine the two measurements, keep track of the result
10:      end for
11:      Choose the position having the highest score
12:    end for
13:  end for
14:  Average the results from each scale
15: end for
```

Here, four Gaussian scales are used with $\sigma = \{1, 2, 3, 4\}$ and corresponding profile widths of $k = \{15, 23, 33, 43\}$ pixels. The search width s is $s = 25$ pixels. The image intensity is transformed to $[0 \dots 1]$ and is weighted equally with the symmetry measure as the two are combined. To reduce the number of irrelevant and erroneous measurements, for instance points outside the cranium, values with a low symmetry measure as well as profiles with low variation are not considered.

The method described above assumes that the scans are roughly aligned. We have also investigated the possibility of maximizing local symmetry along profiles normal to the optimal MSP; however, the results were comparable. The scanline algorithm was therefore favored since it is more foreseeable and easier to implement.

4.2.3. Robust Spline Fitting

As the MSS data is heavily contaminated with outliers, a regular optimization algorithm or regression technique cannot be expected to perform well. Some robust method, capable of handling a large proportion of noise, is therefore needed. Such methods are for instance regression diagnostics, M-estimators, RANSAC and least median of squares.²⁵ In this project, the least median of squares (LMedSq) method is used since it applies well to spline fitting and is capable of handling up to 50 % outliers.²⁵ LMedSq solves the nonlinear minimization problem

$$\min \operatorname{med}_i r_i^2 \quad (10)$$

where r_i denotes the i th residual. Unfortunately, there is no direct solution to this problem. To find the global minimum, an exhaustive search through the entire search space must be performed. For n data points, there are $m_{\text{tot}} = \binom{n}{p}$ ways to choose p points; a number that renders this strategy infeasible in most cases. The common way to overcome this is by considering a selected number $m \ll m_{\text{tot}}$ of samples of p points each. Before we get into details of the algorithm, let's see how it is applied here.

We wish to construct a spline that interpolates or approximates a selected number of control points from our set of data points. To rectify the coordinate system, the data is first rotated according to a least-squares plane fit. The data is roughly planar and the rotation aligns it with the coordinate axes. The in-plane axes are interpreted the xz -plane used in Equation 7. The data points' deviations from the plane are interpreted as the control points y_i . Following the LMedSq algorithm, we wish to find a sample from the data points that produces a spline that gives the lowest possible squared median distance with regards to all data points. The number of data points p to include in each sample is hard to estimate, since we don't have any prior knowledge of the complexity of the MSS. This could be acquired from a training set of mid-sagittal surfaces. Experiments show that choosing between 5 and 9 produces accurate results, and is a reasonable trade-off between low surface complexity and specificity. The remaining question is how to estimate m , the number of random samples to draw. A sample of

p data points is considered good if it does not contain any outliers. Assuming the proportion of outliers is ϵ , the probability that at least one out of m samples is good is

$$P = 1 - (1 - (1 - \epsilon)^p)^m \quad (11)$$

Solving for m gives

$$m = \frac{\log(1 - P)}{\log(1 - (1 - \epsilon)^p)} \quad (12)$$

If our algorithm is to be successful, P should be close to 1. As in ref.,²⁵ P is set to 0.99. What remains to be estimated is ϵ , the proportion of outliers. With the data used in this project, $\epsilon = 0.65$ proved sufficient. The actual proportion of outliers among the data points is lower, probably less than 50%, however, our choice of ϵ also takes into account that a sensible spatial distribution of the sample points is needed. Some samples, despite containing inliers only, have unfortunate positioning of the data points, yielding a malformed spline. To lessen this effect somewhat, samples with co-linear or near co-linear data points are not considered.

The algorithm proceeds by drawing m random sets of p points from the set of all points. For each set, a thin-plate spline is constructed and the squared orthogonal[†] distance from each data point is calculated. The median of these distances is the result for each spline. The spline giving the least median is chosen as the final result.

4.2.4. Other methods for spline fitting

There exist many other appealing and interesting approaches to spline fitting of the MSS. To put the chosen method in perspective, some alternative methods are presented here.

The inter-hemispheric fissure contains cerebral spinal fluid (CSF) which gives a weak MR signal on MPRAGE type scans. The image intensities in this region are therefore low. A straight-forward method is to place a regular grid of control points over the interesting region of a sagittal slice, interpreted as the xz -plane. The control points are allowed to move in the y -direction, and a slice is extracted by thin-plate spline interpolation. The objective function consists of a summation of all pixels in a given slice. Minimizing this function amounts to finding the darkest possible sagittal slice, hopefully representing the optimal MSS. The optimization can furthermore be regularized by combining the intensity-based objective function with a bending energy term. This cost function will try and find an optimal MSS while not introducing excessive bending of the MSS.

Using the data points of Section 4.2.2 it is possible to exchange the sampling technique described above with a standard optimization method such as Nelder-Mead simplex. Again, a regular mesh of control points are placed over an initial sagittal slice and are allowed to move in the y -direction according to some objective function. Experiments with optimization of the median of squared residuals and the sum of squared residuals have been carried out.

5. EXPERIMENTAL RESULTS

5.1. Mid-sagittal Plane Estimation

The mid-sagittal plane was estimated by the method described in Section 4.1 for each of the 62 subjects mentioned in Section 3. The initial MSP, \mathbf{p}_0 , were incident with the center sagittal image-slice, i.e. aligned to the image coordinate system. These initial MSPs are shown in Figure 1. Using a Matlab implementation, a maximum of 100 simplex iterations were carried out on each subject resulting in the optimal MSPs shown in Figure 2. The optimal MSP for subject 20 is shown in detail in Figure 3. The normal width, w , was in the interval [5;15] mm and the spacing of the plane normals were 3 mm.

Qualitative judgement of the appearance of Figure 1 versus Figure 2 gives that the MSP improved in all cases but subject 6. This is solely judged from the amount of cerebral spinal fluid (CSF). Although the change in appearance for subject 6 is very subtle, the initial MSP is preferred over the optimal MSP. This results in a success rate of 98% in the current sample set.

[†]Orthogonal with respect to the coordinate axes, not the spline surface.

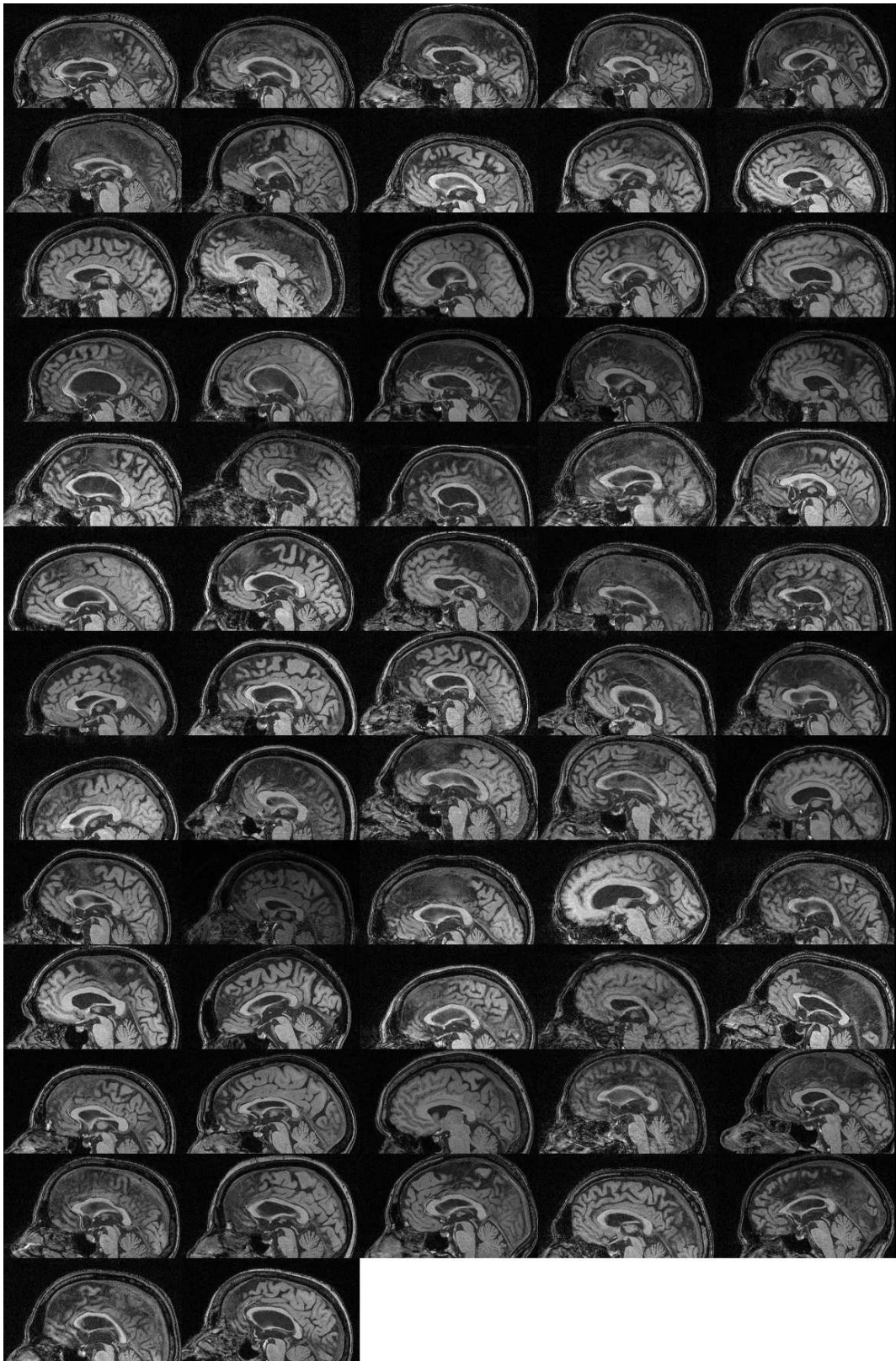


Figure 1. Initial mid-sagittal planes for all 62 subjects (shown row-wise).

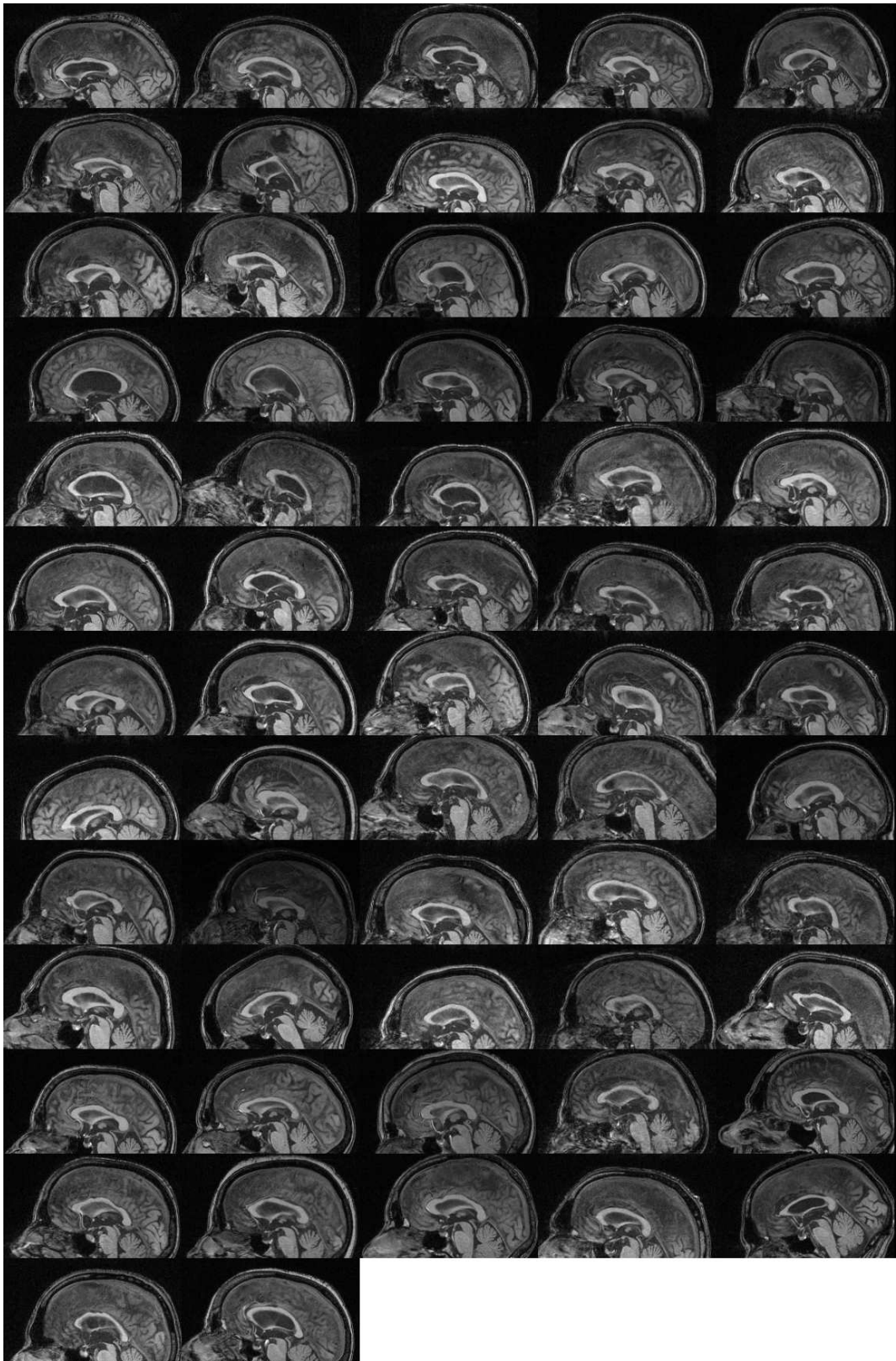


Figure 2. Optimal mid-sagittal planes for all 62 subjects (shown row-wise).

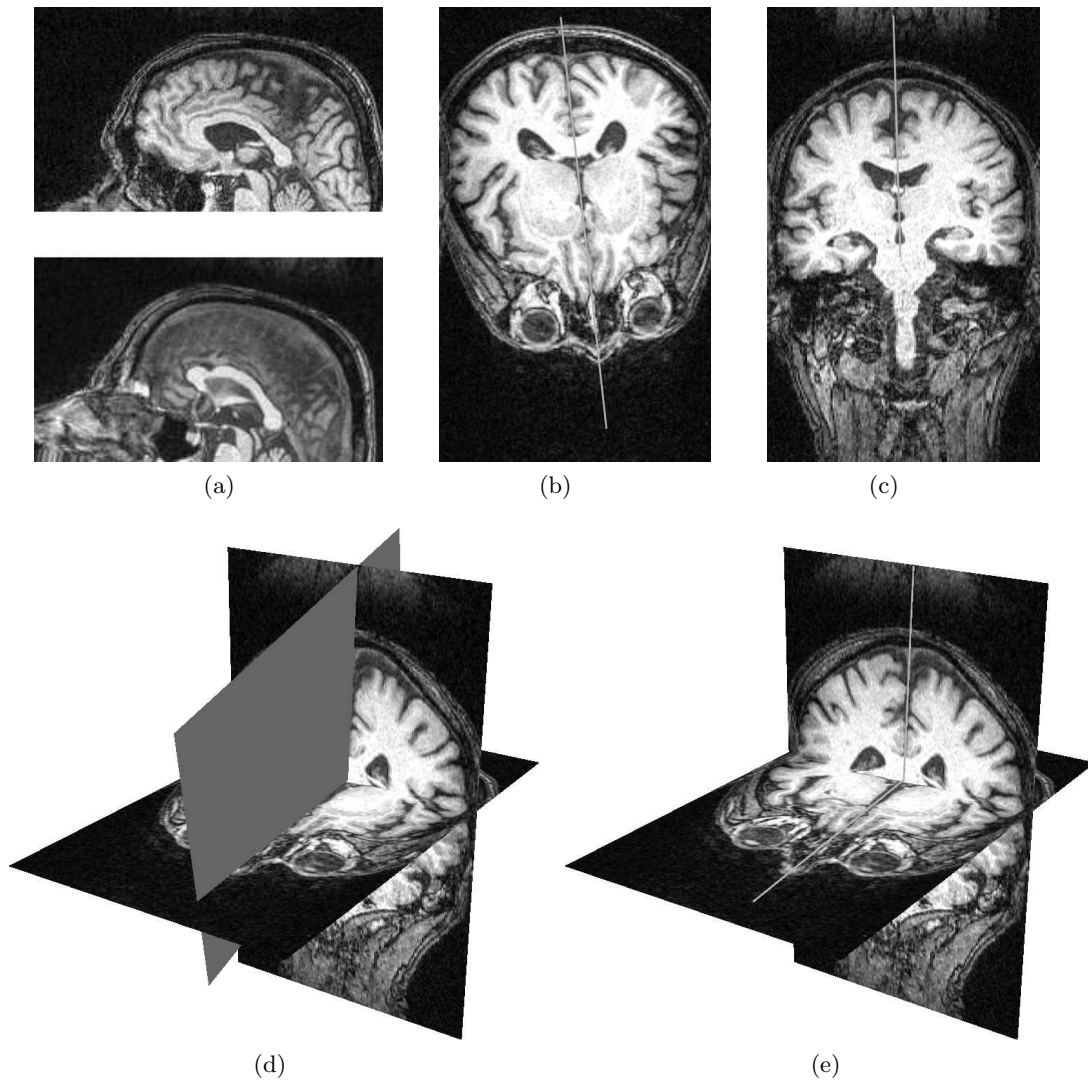


Figure 3. Automatically detected mid-sagittal plane (MSP). (a) Initial (above) and optimal (below) MSP. (b) Axial slice with MSP intersection. (c) Coronal slice with MSP intersection. (d) Axial and coronal slice with estimated MSP. (e) Axial and coronal slice with MSP intersection. All images are contrast-adjusted for optimal display.

5.2. Mid-sagittal Surface Estimation

The LMedSq algorithm is very robust and may give satisfying results for up to 50% outliers.²⁵ However, the data points generated with the algorithm outlined in Section 4.2.2 produces very noisy data when symmetry evidence is weak. As it turns out, this is mainly the case in areas where the MSS deviates from a plane. Still, some evidence of the true MSS remains, and in most cases, the LMedSq algorithm was able to produce satisfying results. Figure 4 shows an example of mid-sagittal surface estimation. At the writing of this article, no quantitative results were available as the data set used contained few examples where the MSS was clearly different from the MSP. Instead, the results of some straight-forward alternatives to the LMedSq method are given below. In relation to these, the LMedSq method was more robust, consistent and conservative in terms of bending of the MSS.

5.2.1. Results of alternative methods

The approach of finding the darkest possible sagittal slice seems to work well at a first glance. The results exhibit satisfyingly low image intensities. However, there is no guarantee that the correct MSS has been found. Some

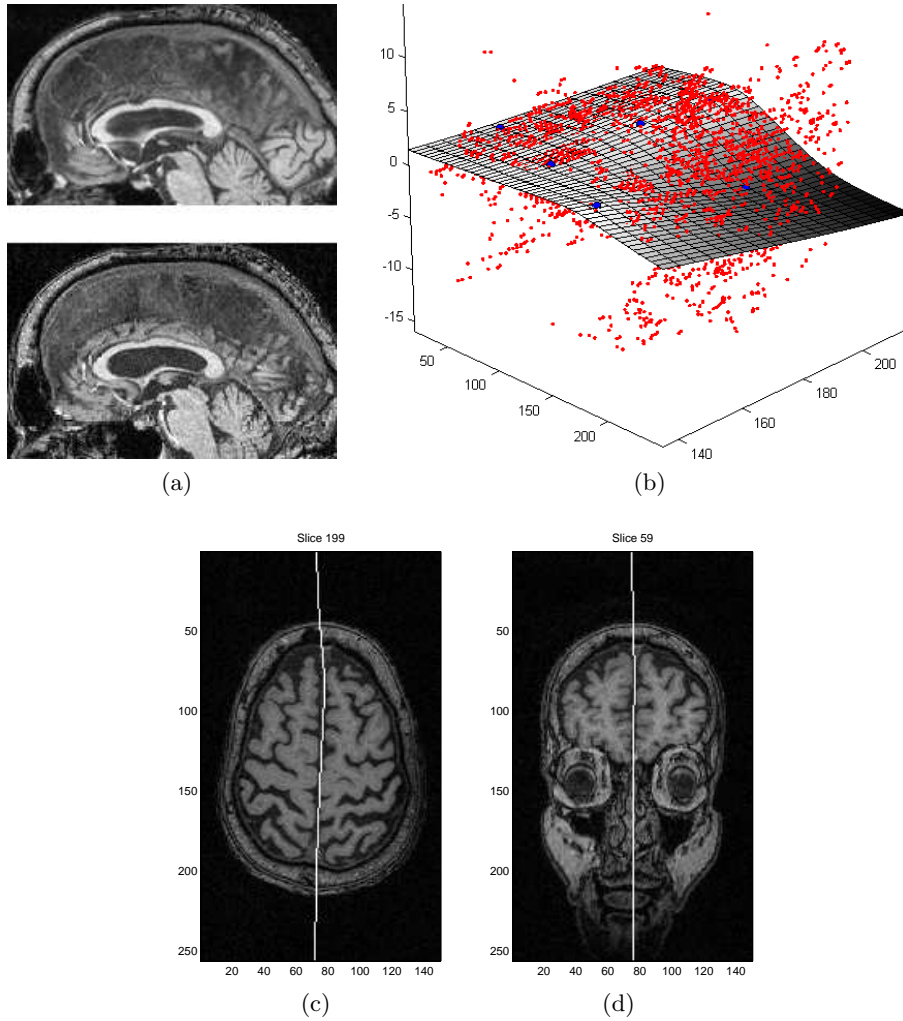


Figure 4. Automatically detected mid-sagittal surface (MSS). (a) Optimal mid-sagittal plane (above) and optimal MSS (below). (b) Points of maximal local symmetry and the optimal MSS based on a robustly estimated, non-interpolating thin-plate spline. (c) Axial slice with MSS intersection. (d) Coronal slice with MSS intersection.

parts of the MSS, e.g. the corpus callosum, consist of white matter leading to high image intensities. The result is that the MSS will move away from these areas into for instance the ventricles. These are areas outside the mid-sagittal fissure also containing CSF giving low MR signal intensities. If such deviations are penalized by introducing a regularization term, the MSS will end up being too constricted, yielding it unable to explain its correct curvature.

For the direct optimization of median squared distance or sum of squared distance from the MSS to the data points, the high proportion of outliers will guide the optimization process into one of the many local minima of the objective function. These experiments clearly show the need for a robust search method such as LMedSq.

6. DISCUSSION

Albeit MSP estimation ultimately should be quantitatively assessed, this preliminary qualitative investigation appears promising. One example out of 62 showed a slight deviation from what is perceived to be the true optimal MSP. However, this deviation may only indicate whether the grader emphasizes on seeing CSF in the frontal or occipital lobe. The results point towards two issues, i) that the method for symmetry estimation expresses

the features wanted in a good MSP estimation, and ii) the optimization approach is stable and accurate in a reasonable large test set. The latter indicates that the proposed method is capable of dealing with typical clinical variation in in-scanner head alignment.

The proposed approach is inherently three-dimensional, conceptually simple and straight-forward to implement. The only independent parameters are the normal width and the normal spacing. In the event of having images with permuted orientation (e.g. coronal and sagittal image slices interchanged) a standard principal axes initialization has been recommended. Due to the local symmetry measure this method is insensitive to partially cropped brains unlike global methods, which heavily relies on the entire head to be scanned. Further, relying on local symmetry rather than the presence of cerebral spinal fluid (CSF) should enable this method to deal with severe variability in inter-hemispheric fissure width, e.g. due to atrophy.⁶ An informal investigation of the fissure width in the present data set supported this observation. In addition, the symmetry approach renders the method insensitive to the choice of MR scanning protocol.

However, the advantages of using a local symmetry come at a cost. Images generated with a very wide impulse-response function (thus having very limited high-frequency content) such as functional SPECT and PET images, will not show any pronounced local symmetry at the inter-hemispheric fissure. For such images our approach will fail. Consequently, the MSP can in such cases only be estimated by educated guesses from global measures such as skull symmetry, regardless of non-coinciding brain and head symmetry and torque effects causing the partitioning surface to curve.¹⁵

There may be doubt about the usefulness of a mid-sagittal surface. For instance, varying curvature of a slice will lead to varying geometric properties, making comparisons and statistical analysis complicated. However, a plane approximation of a curved MSS will result in a partly misplaced cross-section. In effect, there is a trade-off between the complexity of the MSS and the limited accuracy of the MSP.

The LMedSq algorithm works well and is easy to understand and implement. Regarding the complexity of the problem it solves, it has relatively few free parameters that need tuning. However, more results are needed to complete the preliminary findings reported in this paper.

7. CONCLUSION

This paper presented two inherently three-dimensional and novel approaches to estimation of the surface partitioning the hemispheres of the cerebral brain at their point of approximate bilateral symmetry. Contrary to most literature, these employed a local symmetry measure and included partitioning functions being planar as well as general surfaces. Both have been qualitatively validated in a cohort of 62 elderly subjects with encouraging results. Future work will concentrate on assessing their efficiency quantitatively by using synthetic brain data supplemented by manual gold standard measurements on actual MRI. Sensitivity studies with respect to pathologies (e.g. space-occupying lesions), field inhomogeneity and image noise should also be carried out to further validate the current results. The road ahead for mid-sagittal surface extraction contains a mix of sampling a direct optimization to increase efficiency, and an integration of the data point extraction and the search.

Acknowledgements

The work of M. B. Stegmann was supported by The Danish Medical Research Council, grant no. 52-00-0767, and The Danish Research Agency, grant no. 2059-03-0032. Karl Skoglund was supported by The Technical University of Denmark, DTU. Charlotte Ryberg was supported by The Velux Foundation, Denmark.

REFERENCES

1. B. Ardekani, J. Kershaw, M. Braun, and I. Kanuo, "Automatic detection of the mid-sagittal plane in 3-D brain images," *IEEE Transactions on Medical Imaging* **16**(6), pp. 947–52, 1997.
2. A. V. Tuzikov, O. Colliot, and I. Bloch, "Brain symmetry plane computation in MR images using inertia axes and optimization," *Pattern Recognition, 2002. Proceedings. 16th International Conference on* **1**, pp. 516–519 vol.1, 2002.

3. A. V. Tuzikov, O. Colliot, and I. Bloch, "Evaluation of the symmetry plane in 3D MR brain images," *Pattern Recognition Letters* **24**(14), pp. 2219–2233, 2003.
4. J.-P. Thirion, S. Prima, G. Subsol, and N. Roberts, "Statistical analysis of normal and abnormal dissymmetry in volumetric medical images," *Medical Image Analysis* **4**(2), pp. 111–121, 2000.
5. Y. Liu, R. T. Collins, and W. E. Rothfus, "Robust midsagittal plane extraction from normal and pathological 3-D neuroradiology images," *IEEE Transactions on Medical Imaging* **20**(3), pp. 175–192, 2001.
6. D. Wang, J. B. Chalk, D. M. Doddrell, and J. Semple, "Automated detection of mid-sagittal plane in MR images of the head," in *Proceedings of the SPIE - The International Society for Optical Engineering*, **4322**(1-3), pp. 1243–53, SPIE-Int. Soc. Opt. Eng, 2001.
7. A. Lundervold, N. Duta, T. Taxt, and A. K. Jain, "Model-guided segmentation of corpus callosum in MR images," in *Computer Vision and Pattern Recognition*, IEEE Comput. Soc, 1999.
8. F. L. Bookstein, "Landmark methods for forms without landmarks: localizing group differences in outline shape," *Medical Image Analysis* **1**(3), pp. 225–244, 1997.
9. A. Dubb, B. Avants, R. Gur, and J. Gee, "Shape characterization of the corpus callosum in schizophrenia using template deformation," in *Medical Image Computing and Computer-Assisted Intervention - MICCAI*, **2**, pp. 381–388, 2002.
10. M. Brejl and M. Sonka, "Object localization and border detection criteria design in edge-based image segmentation: automated learning from examples," *Medical Imaging, IEEE Transactions on* **19**(10), pp. 973–985, 2000.
11. B. van Ginneken, A. F. Frangi, J. J. Staal, B. M. Ter Haar Romeny, and M. A. Viergever, "Active shape model segmentation with optimal features," *IEEE Transactions on Medical Imaging* **21**(8), pp. 924–933, 2002.
12. M. B. Stegmann, R. H. Davies, and C. Ryberg, "Corpus callosum analysis using MDL-based sequential models of shape and appearance," in *International Symposium on Medical Imaging 2004, San Diego CA, SPIE*, pp. 612–619, SPIE, feb 2004.
13. L. Pantoni, A. M. Basile, G. Pracucci, K. Asplund, J. Bogousslavsky, H. Chabriat, T. Erkinjuntti, F. Fazekas, J. M. Ferro, M. Hennerici, J. O'Brien, P. Scheltens, M. C. Visser, L. O. Wahlund, G. Waldemar, A. Wallin, and D. Inzitari, "Impact of age-related cerebral white matter changes on the transition to disability - the ladis study: Rationale, design and methodology," *Neuroepidemiology* **24**(1-2), pp. 51–62, 2005.
14. S. Prima, S. Ourselin, and N. Ayache, "Computation of the mid-sagittal plane in 3D medical images of the brain," tech. rep., Institut National de Recherche en Informatique et en Automatique - INRIA Sophia Antipolis, 1999.
15. S. Prima, S. Ourselin, and N. Ayache, "Computation of the mid-sagittal plane in 3D medical images of the brain," in *Proceedings of the Medical Imaging Computing and Computer Assisted Intervention Conference (MICCAI 2000)*, *Lecture Notes in Computer Science* **1843**, pp. 685–701, Springer Verlag, 2000.
16. Y. Liu, R. Collins, and W. E. Rothfus, "Evaluation of a robust midsagittal plane extraction algorithm for coarse, pathological 3D images," in *Proceedings of the Medical Imaging Computing and Computer Assisted Intervention Conference (MICCAI 2000)*, *Lecture Notes in Computer Science* **1935**, pp. 83–94, (Pittsburgh, PA), October 2000.
17. J. Mykkänen, J. Töhma, J. Luoma, and U. Ruotsalainen, "Automatic extraction of brain surface and mid-sagittal plane from PET images applying deformable models," tech. rep., Institute of Signal Processing, Tampere University of Technology, Finland, 2003.
18. G. E. Christensen, H. Johnson, T. A. Darvann, N. V. Hermann, and J. L. Marsh, "Midsagittal surface measurement of the head: A quantitative assessment of craniofacial asymmetry," in *International Symposium on Medical Imaging 1999, Proc. of SPIE vol. 3661*, K. M. Hanson, ed., pp. 612–619, SPIE, 1999.
19. T. A. Darvann, H. Johnson, G. Christensen, J. L. Marsh, N. V. Hermann, Y. O. Kim, A. A. Kane, S. Kreiborg, and F. W. Zonneveld, "A new tool for visualization and quantification of the midsagittal plane in the human skull," in *Oral presentation/abstract at the 56th Annual Meeting of the American Cleft Palate - Craniofacial Association*, 1999.
20. M. B. Stegmann and R. H. Davies, "Automated analysis of corpora callosa," Tech. Rep. IMM-REP-2003-02, Informatics and Mathematical Modelling, Technical University of Denmark, DTU, mar 2003.
21. W. H. Press, S. A. Teukolsky, W. T. Vetterling, and B. R. Flannery, *Numerical Recipes in C: The Art of Scientific Computing*, Cambridge University Press, second ed., 1992.
22. G. Donato and S. Belongie, "Approximate thin plate spline mappings," in *Computer Vision - ECCV 2002. 7th European Conference on Computer Vision. Proceedings, Part III (Lecture Notes in Computer Science Vol.2352)*, A. Heyden, G. Sparr, M. Nielsen, and P. Johansen, eds., pp. 21–31, Springer-Verlag, 2002.
23. J. T. Kent and K. V. Mardia, "The link between kriging and thin plate splines," *Statistics and optimisation*, pp. 324–339, 1994.
24. I. L. Dryden and K. V. Mardia, *Statistical Shape Analysis*, John Wiley & Sons, 1999.
25. Z. Zhang, "Parameter estimation techniques: a tutorial with application to conic fitting," *Image and Vision Computing* **15**(1), pp. 59–76, 1997.